

Article

Analogue Application of Behaviour and Transport of Naturally Occurring Strontium in Cold-Region Aquatic Environments to ^{90}Sr

Enisa Zanicic ^{1,2,*} and Dena W. McMartin ^{1,3} 

¹ Environmental Systems Engineering, University of Regina, Regina, SK S4S 0A2, Canada; dena.mcmartin@uleth.ca

² Integrated Water Systems, Regina, SK S4S 0A2, Canada

³ Geography and Environment, University of Lethbridge, Lethbridge, AB T1K 3M4, Canada

* Correspondence: integratedwaters@gmail.com; Tel.: +1-(306)-690-4995

Abstract: Quantification and scientific observations of the fate and transport of dissolved strontium in water systems, particularly cold climate water systems, are severely lacking. In this work, in an experiment conducted at a temperature of 6 °C, the observation of strontium precipitation along with calcium carbonate minerals from cold wastewater is investigated. ICP-MS is used for metal analyses where the distribution of the species and saturation state of minerals along with a surface complexation model was performed using the public-use USGS geochemical modeling software, PHREEQC (PH Redox Equilibrium (in C language)). Sample media were analyzed using XPS and Raman spectroscopy. The results suggest that the loss of strontium from natural waters is via the process of co-precipitation with calcite, a calcium carbonate polymorph. The observations and findings are intended to be useful to quantify the loss of ^{90}Sr from the water, in the case of an unplanned release from a nuclear reactor-operated facility. The results indicate that the precipitation model is a robust and reliable approach to predicting and monitoring the behaviour and transport of strontium that may occur in natural environments as a result of an accidental nuclear release.

Keywords: strontium; radionuclides; aqueous transport; cold climate



Citation: Zanicic, E.; McMartin, D.W. Analogue Application of Behaviour and Transport of Naturally Occurring Strontium in Cold-Region Aquatic Environments to ^{90}Sr . *Environments* **2022**, *9*, 72. <https://doi.org/10.3390/environments9060072>

Academic Editor: Yu-Pin Lin

Received: 19 April 2022

Accepted: 7 June 2022

Published: 15 June 2022

Publisher's Note: MDPI stays neutral with regard to jurisdictional claims in published maps and institutional affiliations.



Copyright: © 2022 by the authors. Licensee MDPI, Basel, Switzerland. This article is an open access article distributed under the terms and conditions of the Creative Commons Attribution (CC BY) license (<https://creativecommons.org/licenses/by/4.0/>).

1. Introduction

One of the challenges in quantifying, understanding, and predicting the behaviours of radioactive substances that are non-gamma emitters such as ^{90}Sr in the natural environment is in data collection, where the use of complex and time-consuming radiochemical procedures is required to assess the substances [1]. For those reasons, the behaviour of strontium in the cold surface water is either under-studied or under-reported in the scientific and engineering literature. In general, strontium is very reactive and readily oxidizes to the plus two oxidation state [2]. The chemical behaviour of radioactive isotope Sr^{90} is identical to the stable isotopes of strontium found in nature. The presence of chemically neutral extra neutrons in Sr^{90} nuclei is what makes them unstable, hence radioactive. Improving the understanding of the behaviour of Sr^{2+} in water under cold conditions supports the scientific knowledge and prediction of how Sr^{90} might behave in Canadian and other cold-climate aquatic environments if it is accidentally released. The chemical reduction of dissolved strontium in surface water occurs by adsorption and/or precipitation [2–4].

When radionuclides enter an aqueous receiving environment by atmospheric deposition and/or direct entry, they are present as particles of various sizes and distributions, structures, and oxidation states [5,6]. Atmospheric deposition on land may contribute to surface water contamination in the case of overland flows and runoff, via percolation, water- or wind-induced erosion, or sedimentation. Radionuclides that are transported to surface waters are moved to the lower parts of watersheds by advective transport where they

accumulate in sediments and bioaccumulate in flora and fauna. Accumulation of radionuclides in sediments and biota is significantly amplified by climate change. For example, when combined with climate projections for the study region, shallow lakes are expected to lose volume to evaporation and gain heat more rapidly than in the past [7]. As the water temperature increases, so does the bioaccumulation of particles such as strontium [8]. Projections for reduced precipitation in summer along with increased water evaporation increase the salinity of the remaining water, which, in turn, affects the concentration of radionuclides by influencing solubility, adsorption, and desorption to the sediments, and accumulation in aquatic flora and fauna. It determines the balance in radionuclides distribution between the water and the aquatic ecosystem [9]. Microbial activity can also affect the dispersion mechanisms and bioavailability of radionuclides by changing chemical speciation, solubility, and sorption properties [10]. Prime examples of such mechanisms are cooling ponds at the Chernobyl Nuclear Power Plant, for instance. In the ponds, anoxic and slightly alkaline conditions created an environment in which there is a low particle weathering rate and remobilization of radionuclides in sediment [11].

At a nuclear power facility, in the case of an unplanned release, ^{90}Sr , ^{137}Cs , and iodine isotopes are of the most radiological concern since they can be inhaled and deposited in living tissues. The isotopes of ^{90}Sr and ^{137}Cs are fission products found in nuclear reactor core materials and the fallout from nuclear testing material. While ^{137}Cs and iodine isotopes are well studied, ^{90}Sr is less so. ^{90}Sr is a short-lived radionuclide and one of the most hazardous pollutants to humans. Its half-life is 29.8 years, and its decay occurs with high particle beta emission. ^{90}Sr decays to ^{90}Y , which has a half-life of 64 h and a very high beta emission energy. In the natural environment, radionuclides are similar to organic pollutants in the sense that they sorb to particulates. However, being inorganic, they are not subject to the same processes and mechanisms of decomposition as organics. The adsorption and desorption of radionuclides by the surface bed sediments are the main chemical exchange process. Those processes are not always reversible and are subject to geochemistry. The exchange of radionuclides between water and sediments, in general, is due to the perturbation of sediments, and to a degree, the uptake and excretion of radionuclides by aquatic biota. The applicability of stable isotopes as important tracers and markers continues to evolve and is viewed as a constructive and safe method for monitoring and modeling radionuclide fate in natural environments [12–14].

It is a common practice to use stable isotopes as a tracer that aid in following the fate of compounds in intricate systems [15] (IAEA, 2009). Strontium (^{87}Sr) is an alkaline-earth metal and can serve as an analogue or surrogate to ^{90}Sr detection in the natural environment. In particular, the isotopic ratio of $^{87}\text{Sr}/^{86}\text{Sr}$ is routinely used as a tracer for groundwater studies in which the fate and transport of radionuclides are modeled [16,17]. In nature, Sr^{2+} is not present in a free form as it reacts readily with water and oxygen. It forms compounds with other elements and minerals such as celestite (SrSO_4) and strontianite (SrCO_3). Laboratory studies report strontium removal with aragonite and calcite, with published results suggesting that aragonite is more effective than calcite for mediating strontium removal from water [18,19]. Dissolved in water, strontium will co-precipitate with calcium carbonate as an impurity in calcite precipitate. Co-precipitation might occur as inclusion in homogenous crystal formation, occlusion of impurities scattered through the crystal, or surface adsorption of impurity ions by precipitate [19]. Several factors including the depth of the overlaying water, sediment geochemistry, and physiochemical conditions will govern the pollutant retention within the sediments [20].

The objective of this research was to identify methods for monitoring and quantifying naturally occurring strontium in cold-region water sources. Understanding the behaviour of naturally occurring strontium in water and sediments will assist in establishing a robust monitoring approach required to assess ^{90}Sr fate and transport in the event of an unplanned release from the eventual operation of nuclear-fueled power plants in the region.

2. Materials and Methods

The benefit of performing work in the field or a non-lab-controlled environment is results that are a reflection of natural processes and can be applied commonly with minimal adjustments, where lab-controlled results are often produced by using pure materials and/or higher pressures that are not part of the natural processes. Therefore, a field monitoring and quantification experiment was completed using wastewater collected from a cold-region water treatment plant (WTP) using a ground water source. This source water has a large amount of natural strontium. Consequently, reverse osmosis brine wastewater produced at the plant contains a high concentration of strontium. Accordingly, the planning of the experiment proceeded with the objective to determine the co-precipitation constant that can be used to empirically model and predict the mechanisms controlling the solubility, transport, and bioavailability of strontium in water.

2.1. Study Region

The Canadian province of Saskatchewan is a land-locked prairie province, with a diverse climate ranging from sub-arctic in the north to humid continental and semi-arid in the south (Figure 1) [21]. The soils and ground water aquifers in Saskatchewan contain naturally occurring radionuclides including uranium, strontium, and radium in significant concentrations.

Most of the strontium in water is in the dissolved form (total \approx dissolved) [22]. In Saskatchewan, the freshwater concentrations of total strontium range from 0.029 mg/L to 1.74 mg/L with a median of 0.34 mg/L. In ground water, the median level is 0.63 mg/L with a maximum level of 2.1 mg/L [22]. The federal guidelines for surface water quality objectives for the protection of aquatic life for dissolved strontium is 2.5 mg/L [23].

In this specific study, the source ground water is from the Hatfield Aquifer and contains naturally occurring strontium. The water in the aquifer is highly mineralized, containing ammonia, high sulfates, iron, arsenic, and manganese (Table 1).

2.2. Field Samples: Water and Sediments

An experiment was designed to observe the Sr^{2+} reduction pathway in wastewater open to the atmosphere and at low temperatures. The anticipated pathway for strontium reduction from surface water is strontium co-precipitation with calcium carbonate (CaCO_3) polymorphs by means of strontium incorporation into the CaCO_3 precipitate. The WTP wastewater discharged in holding ponds was used as a source of water, and pyrolusite media was used for adsorption/precipitation. Monthly monitoring of the wastewater quality in holding ponds was in durations greater than 24 months.

Monthly sampling of 300 mL of water in plastic bottles for general chemicals and total dissolved solids analyses was performed at both the inlet and outlet of the ponds. Additional samples for ammonia and metals analyses were collected in 80 mL plastic bottles with 0.1 M of nitric acid and 100 mL glass bottles with 0.1 M of nitric acid, respectively. Samples were stored in a cooler at approximately 4 °C and shipped to a lab for analysis within 24 h of collection. Water samples were analyzed for conductivity, pH, total dissolved solids (TDS), total suspended solids (TSS), alkalinity, chloride, fluoride, ammonia, nitrate, nitrite, sulfate, and total and dissolved metals at an accredited QA/QC-certified laboratory.

Holding ponds' sediment analyses were completed to determine the presence and precipitation of strontium through the ponds. Samples were collected in five holding ponds over a period of 2 months in summer. Sediment collection comprised randomized location selection (based, in large part, on safety and accessibility) and scooping of the top layer to a depth of 15 cm to produce 2 L of sample per location. Sediments were stored at 4 °C in 2 L plastic bags and transported within 48 h for analysis. Sediment analysis for total metals was conducted as per EPA 3050, using inductively coupled plasma mass spectrometry (ICP-MS).

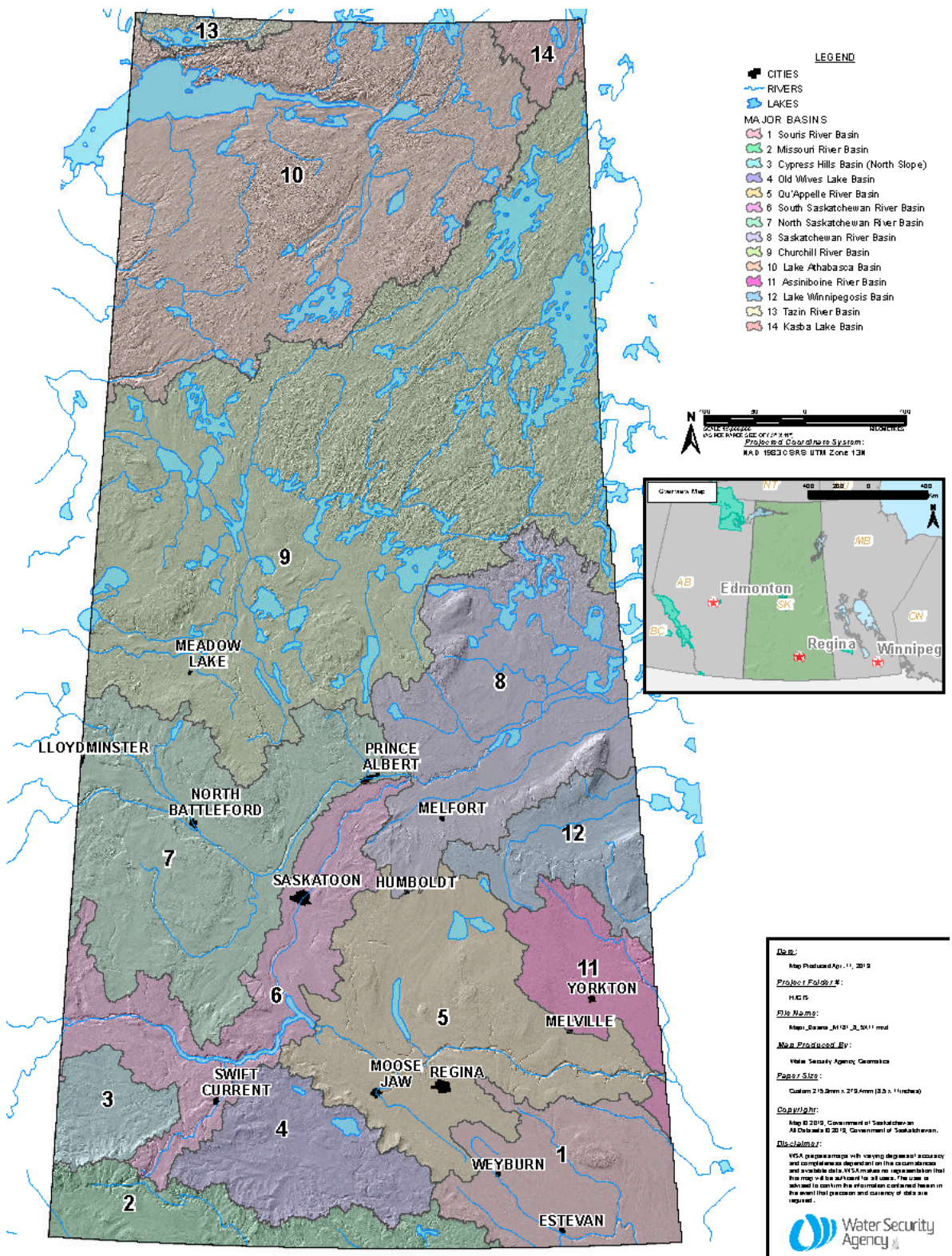


Figure 1. Map of Saskatchewan watersheds and water bodies [24].

Table 1. Hatfield aquifer source water quality.

Parameter	Unit	Lowest Detection Limit	Ground Water (Summer)
Conductivity	uS/cm	5.00×10^0	1.93×10^3
pH	pH	1.00×10^{-1}	7.83×10^0
Total Dissolved Solids	mg/L	2.00×10^1	1.40×10^3
Alkalinity, Total (as CaCO ₃)	mg/L	5.00×10^0	4.22×10^2
Ammonia, Total (as N)	mg/L	5.00×10^{-2}	2.40×10^0
Bicarbonate (HCO ₃)	mg/L	6.10×10^0	5.15×10^2
Carbonate (CO ₃)	mg/L	5.00×10^0	<5.0
Chloride (Cl)	mg/L	2.50×10^0	8.60×10^1
Manganese (Mn)	mg/L	2.00×10^{-4}	5.80×10^{-1}
Iron (Fe)	mg/L	1.00×10^{-2}	1.52×10^0
Barium (Ba)-Total	mg/L	1.00×10^{-4}	9.70×10^{-3}
Calcium (Ca)-Total	mg/L	5.00×10^{-2}	1.19×10^2
Magnesium (Mg)-Total	mg/L	5.00×10^{-3}	5.70×10^1
Potassium (K)-Total	mg/L	5.00×10^{-2}	1.20×10^1
Sodium (Na)-Total	mg/L	5.00×10^{-2}	2.34×10^2
Sulfate (SO ₄)	mg/L	1.50×10^0	5.30×10^2
Uranium (U)-Total	mg/L	1.00×10^{-5}	1.60×10^{-3}

The calculation of the distribution of species and a saturation state of the wastewater was completed using PHREEQC (PH Redox Equilibrium (in C language)). The PHREEQC diffuse double-layer surface-complexation model was used to equilibrate the WTP wastewater with sediments/colloids in the ponds. PHREEQC analysis was further used to determine the saturation of the chemical species in raw water samples via the saturation index (SI) method. The PHREEQC calculation of the distribution of species and the saturation state of the wastewater, relative to the set of minerals in the wastewater, along with modeling mineral adsorption to the surfaces particles such as sediment particles and colloids in the ponds, was performed using the surface complexation model based on the Dzombak and Morell [25] database for the complexation of heavy metal ions on hydrous ferric oxide.

2.3. Laboratory Experimental Design and Analyses

A lab experiment was completed to supplement field observations and advance our knowledge of how strontium interacts with pyrolusite, the manganese oxide media. First, three treatments of pyrolusite were prepared including raw, humic acid (HA)-coated, and fulvic acid (FA)-coated media. Here, 100 ± 0.2 g of solid manganese dioxide media (pyrolusite) from the AWI Company was thoroughly washed in deionized water five times to remove fines. Then, 300 ± 10 mg of HA from Sigma-Aldrich was dissolved in 50 mL of 0.01 M NaOH. The final HA concentration was 6 ± 0.2 g/L. Additionally, 5 mg of 95% pure FA from MP Biomedicals was dissolved in 5 mL of methanol. The mixture was shaken for 3 h at 25 °C to dissolve the FA and produce a final FA concentration of 1 ± 0.05 g/L. Twenty grams (20 g) of pyrolusite was placed in each of three 0.5 L glass beakers to which 200 mL of distilled water was added. In Beaker 1, no HA or FA was added to produce an experimental control. Beaker 2 contained 0.5 mL of the FA mixture (or 100 mg in solution) and was stirred for 15 min to expose the media to the water mixture. In Beaker 3, 0.5 mL of the HA mixture was added and stirred as above to produce a solution containing 300 mg

of HA. The media was soaked for 10 h at 25 °C; the beakers were stirred for 2–3 min every 2 h to maximize contact between the water and media.

In the pyrolusite media sorption experiments, raw water from the wastewater holding ponds was collected in 4 L plastic bottles. The bottles were rinsed with raw water to minimize minerals' adsorption from the collected water onto the bottles. Wastewater samples were collected at the exit of Pond 1 and entrance to Pond 2 (Figure 2). Because of ice and snow cover at the time of sampling, an ice-free location was selected to capture representative aliquots of flowing water.



Figure 2. WTP wastewater holding ponds with flow of water in the direction of ponds 1 through 5. Samples for laboratory experiments were collected at the location identified with the red arrow. Pond depths range from 1–2 m with each pond capable of retaining a maximum of 5000 m³ of WTP wastewater; retention time is calculated at 3–5 d depending on time of year and consumption rates. The ponds were originally constructed in the 1970s to provide physical settling of suspended solids and consumption of free chlorine residuals. Holding ponds were covered in ice and snow at the time of sample collection.

Samples were immediately filtered on-site using 0.4 µm GF/C filters, and 1 L of filtered water was used to rinse the plastic sample bottles. Another 10 L of filtered water was collected and stored at 4 °C for less than 24 h prior to use. One filtered sample was submitted for chemical parameter analysis as a reference sample.

In the laboratory, six 1 L glass beakers were rinsed three times with distilled water and twice with filtered sample water to minimize mineral adsorption onto the beakers during experiments. To each beaker, 10 g of the prepared pyrolusite media was added. Two beakers were prepared with raw media, 2 with HA pretreated pyrolusite, and 2 with FA-pretreated pyrolusite. One litre (1 L) of filtered pond water was added to all 6 beakers, and the mixture was paddle-stirred continuously at 70 rpm for 6 h. A temperature of 6 °C was maintained throughout the 3-day experiment. Water samples of 100 mL and pyrolusite media samples of 1 g were collected at 0.5, 3, and 6 h and at the conclusion of the 3-day experiment. The concentrations of dissolved metals in water samples were determined from samples that were collected in glass bottles and preserved with 0.1 M nitric acid.

The full general chemicals analysis was completed only with 6-h samples, including those provided in Table 1.

The 1 g pyrolusite media samples collected at 3 h and 3 d were subjected to X-ray photoelectron spectroscopic (XPS) analysis at the Saskatchewan Structural Sciences Centre at the University of Saskatchewan. XPS provides quantitative and chemical state analysis relating to the media surface. Because each element has a unique binding energy, XPS is used to identify and determine the concentration of individual elements sorbed to the surface of the media. If neither Sr^{2+} adsorption or precipitates were observed, it was presumed that the incorporation of the Sr^{2+} in calcium carbonate precipitate was a significant factor in the initial Sr^{2+} loss from the water phase. To confirm that hypothesis, Raman Spectroscopy analysis was then conducted using a Reinshaw Raman Invia Reflex Microscope at the University of Saskatchewan, Saskatchewan Structural Sciences Centre. Raman spectroscopy measures light scattering to elucidate molecular structures, including the presence of and interactions with polymorphs [26]. The differences that arise from the structural arrangement and site symmetries of the molecules in calcite and aragonite provide the basis for differentiation between the polymorphs.

Previous research demonstrated the use of Raman Spectroscopy to determine Sr/Ca ratios [27] and to determine crystalline lattice bands for aragonite, calcite, whiterite, and strontianite [28]. These data and the RRUFF database [29] containing structural, spectroscopic, and chemical minerals identification data of over 70% of the known minerals were used to quantify interactions on the 3 preparations of pyrolusite media in this research. The objective of Raman Spectroscopy analysis was to identify (a) precipitates forming at the initial contact between water and media and (b) the nature of those precipitates. If the precipitates are calcium carbonates, the polymorph type and nature of the impurities can be determined based on the vibrational frequency peaks (Figure 3) [29].

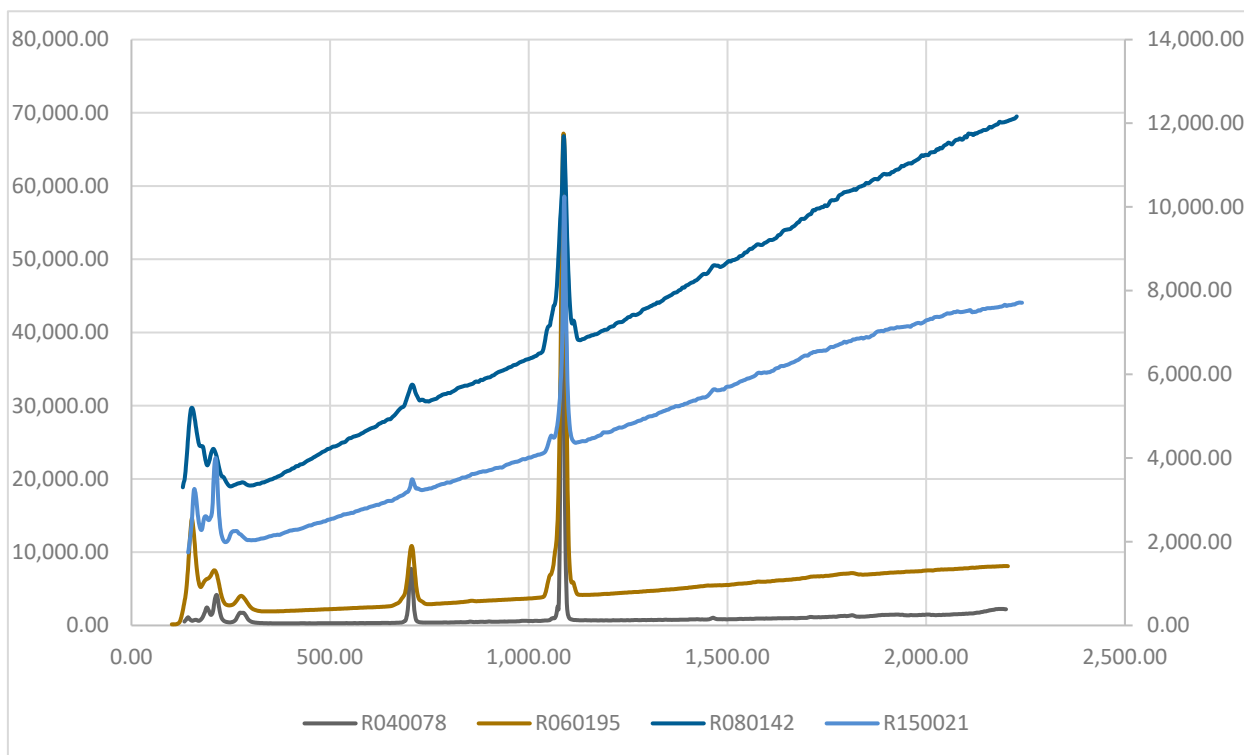


Figure 3. RRUFF aragonite database spectra, where R040078 and R060195 are pure aragonite (gray and gold), R150021 aragonite contains 98.7% of calcium and 0.96% strontium (light blue), and R080142 aragonite contains 96% calcium and 2% strontium (dark blue).

Samples were examined at 50× and 20× amplification using the laser specifications shown in Table 2.

Table 2. Raman Spectroscopy laser power measured at the sample for 20× and 50×.

Objective	514.5 nm Ar Laser (100% LP) LP @ Laser Head = 10.00 mW	Working Distance (mm)
20×/0.40 NPLAN	3.59	1.1
50×/0.75 NPLAN	2.74	0.37

3. Results and Discussion

3.1. Field Samples: Water and Sediments

The source ground water used in this research is high in dissolved minerals, sulfates, iron and manganese, and ammonia. As such, reverse osmosis brine (75% plant recovery produces 4 times concentrated wastewater brine) water is oversaturated with CaCO_3 , and excess CaCO_3 precipitates as the water moves through the ponds and interacts with the environment. Precipitation of the minerals occurs as the water is continuously striving toward equilibrium. The water quality changes as it passes through the various ponds, including physical settling, wetland plant and soil interactions, and biogeochemical aging across the five-pond system (Table 3). The five-pond design ensures that WTP wastewater is sufficiently treated to allow for discharge to the aquatic receiving environment, which, in this case, is a disposal well that returns treated wastewater to the Hatfield Aquifer.

Table 3. General chemistry analysis WTP wastewater entering and leaving the ponds as sampled in spring (May) and winter (December). Samples were collected within an hour of each other.

Parameters	Unit	Inlet (Spring)	Inlet (Winter)	Outlet (Spring)	Outlet (Winter)
Conductivity	$\mu\text{S}/\text{cm}$	5.37×10^3	4.79×10^3	3.36×10^3	3.87×10^3
pH	pH	7.75×10^0	7.89×10^0	7.99×10^0	7.91×10^0
Total Dissolved Solids (TDS)	mg/L	4.92×10^3	4.05×10^3	2.76×10^3	2.89×10^3
Alkalinity, Total (as CaCO_3)	mg/L	1.09×10^3	1.09×10^3	6.23×10^2	7.55×10^2
Ammonia, Total (as N)	mg/L	6.78×10^0	5.30×10^0	6.10×10^{-1}	2.20×10^0
Chloride (Cl)	mg/L	2.04×10^2	1.60×10^2	1.26×10^2	1.37×10^2
Iron (Fe)-Total	mg/L	<0.05	<0.05	7.30×10^{-1}	4.51×10^{-1}
Calcium (Ca)-Total	mg/L	4.80×10^2	4.43×10^2	2.68×10^2	3.10×10^2
Magnesium (Mg)-Total	mg/L	2.50×10^2	2.60×10^2	1.65×10^2	1.85×10^2
Manganese (Mn)-Total	mg/L	5.00×10^{-2}	3.00×10^{-2}	9.10×10^{-1}	1.54×10^0
Potassium (K)-Total	mg/L	2.50×10^1	2.37×10^1	2.09×10^1	1.90×10^1
Strontium (Sr)-Total	mg/L	4.06×10^0	3.57×10^0	1.95×10^0	2.27×10^0
Sulfur (as SO_4)	mg/L	2.26×10^3	2.02×10^3	1.34×10^3	1.54×10^3
Sodium (Na)	mg/L	6.26×10^2	4.97×10^2	3.69×10^2	3.91×10^2

In general, the WTP effluent quality meets the regulatory guidelines for particulates and ammonia, and reductions of other parameters, such as TDS, are evident. Only total metals data are provided since total and dissolved concentrations were statistically the same. Water quality discharged from the WTP into the holding ponds contains significantly higher concentrations of minerals than that discharged from the ponds (Table 3). The difference in the concentration of minerals is partially due to the precipitation and surface runoff. However, the reduction in mineral content can also be noted in the months when ponds are covered with ice and there is no external dilution. For both the spring and

winter water samples, saturation index analyses were performed using PHREEQC (Table 4). The results indicate that precipitation of only calcium carbonate species and dolomite is expected. Therefore, a loss of calcium and magnesium from the water contributed to precipitation from the water in the ponds.

Table 4. Saturation Index values for WTP wastewater quality at two holding pond sampling locations (inlet and outlet) and for raw water control and untreated pyrolusite laboratory experiment samples.

Saturation Index (SI)					
Phase	Formula	Inlet	Outlet	Control	Untreated 6 h
Anhydrite	CaSO ₄	-5.70×10^{-1}	-8.80×10^{-1}	-7.20×10^{-1}	-7.60×10^{-1}
Aragonite	CaCO ₃	1.17×10^0	1.02×10^0	1.44×10^0	1.34×10^0
Calcite	CaCO ₃	1.33×10^0	1.18×10^0	1.60×10^0	1.50×10^0
Celestite	SrSO ₄	-4.50×10^{-1}	-8.60×10^{-1}	-7.10×10^{-1}	-7.20×10^{-1}
Dolomite	CaMg(CO ₃) ₂	2.44×10^0	2.20×10^0	2.99×10^0	2.79×10^0
Gypsum	CaSO ₄ :H ₂ O	-5.00×10^{-2}	-3.60×10^{-1}	-2.00×10^{-1}	-2.40×10^{-1}
Halite	NaCl	-5.62×10^0	-6.00×10^0	-5.77×10^0	-5.85×10^0
Strontianite	SrCO ₃	-1.20×10^{-1}	-3.60×10^{-1}	-4.00×10^{-2}	-3.00×10^{-2}
Sylvianite	KCl	-6.46×10^0	-6.71×10^0	-6.62×10^0	-6.72×10^0

The saturation index (SI) for gypsum and strontianite for waste entering the ponds is close to zero, implying that precipitation is unlikely, where that at the exit is negative suggesting undersaturation of the species with no precipitation expected. For both water samples and locations, the SI for anhydrite is negative indicating there will be no precipitation. Additionally, the PHREEQC model for diffuse double-layer surface complexation, using the pre-brine inlet data, showed that metal oxide particles in the water will attract some of the minerals to adsorb to the surface of the particles.

The results of sediment analysis of calcium, magnesium, sodium, and sodium adsorption ratio (SAR) values are summarized for each pond (Table 5).

The data show that the concentration of sodium was higher than that of calcium and magnesium prior to a change in operations at the WTP that resulted in daily brine discharge occurring after the first set of samples had been collected and had been in operation for those collected approximately 2 years after that operations change. Specifically, the change in operations at the WTP was the removal of the electro dialysis reversal (EDR) plant and surface water filter units. Currently, the WTP consists of Green Sand plus filters and reverse osmosis filtration units. While in the past the brine from EDR was sent to deep groundwater wells and backwash water from the filters was returned to the ponds, the current method for disposal is to discharge brine from the RO units along with Green Sand, plus filter backwash to the ponds. Prior to daily brine discharge, sediments exhibited a higher sodium adsorption ratio (SAR).

Community growth and stringent regulatory requirements, especially disinfection by-products, forced the community to upgrade WTP to produce potable water that is safe and stable. In the past, water instability was amplified by chlorine decay and disinfection by-product formation due to the organics in the water and distribution system. Customers would not only receive water high in trihalomethanes and haloacetic acid, but also low in free chlorine levels. Today, the plant is optimized so that customers receive safe potable water, and there is no visible/quantifiable impact on the distribution system.

Table 5. Pond sediment analysis: Sediments collected (a) prior to daily brine discharge and (b) approximately 2 years after the start of routine brine discharge. Samples collected as post-brine 1 and 2 were collected approximately 1 month apart during summer.

Parameter (mg/kg)	Date	Pond Cells (Saturated Paste Extractables)				
		P1	P2	P3	P4	P5
Calcium	Pre-Brine	4.52×10^2	4.58×10^2	6.74×10^2	3.90×10^2	5.15×10^2
	Post-Brine 1	1.25×10^3	1.55×10^3	2.98×10^2	1.46×10^3	4.89×10^2
	Post-Brine 2	1.26×10^3	1.02×10^3	9.52×10^2	1.62×10^3	6.92×10^2
Magnesium	Pre-Brine	1.08×10^2	2.44×10^2	2.54×10^2	2.18×10^2	1.87×10^2
	Post-Brine 1	6.79×10^2	1.15×10^3	1.89×10^2	8.88×10^2	3.52×10^2
	Post-Brine 2	5.81×10^2	7.24×10^2	5.56×10^2	9.41×10^2	4.51×10^2
Sodium	Pre-Brine	6.40×10^2	9.97×10^2	1.13×10^3	9.19×10^2	8.72×10^2
	Post-Brine 1	1.77×10^3	2.84×10^3	4.52×10^2	2.24×10^3	8.32×10^2
	Post-Brine 2	1.87×10^3	1.88×10^3	1.43×10^3	2.47×10^3	1.13×10^3
SAR	Pre-Brine	5.69×10^0	8.12×10^0	8.03×10^0	7.73×10^0	7.02×10^0
	Post-Brine 1	5.44×10^0	6.03×10^0	5.13×10^0	5.83×10^0	4.72×10^0
	Post-Brine 2	6.06×10^0	6.00×10^0	4.74×10^0	6.08×10^0	5.07×10^0

In both post-brine samples, despite the increase in Na^- deposition through the ponds, SAR for all ponds decreased due to elevated Ca^{2+} and Mg^{2+} concentrations in the sediments most likely due to precipitation from the WTP wastewater. For example, the SAR in Pond 1 did not change significantly, but SAR in Pond 2 experienced a reduction from 8 to 6, sodium concentration increased from 997 mg/kg to more than 2000 mg/kg, and calcium and magnesium increased from 458 mg/kg to >1000 mg/kg on average and 244 mg/kg to ~1000 mg/kg on average, respectively, following 2 years of daily brine discharge.

The metal analysis of pond sediments (Table 6) shows that aluminum and calcium dominate, likely as a function of many years of aluminum-based WTP coagulant use. The even distribution of iron and manganese is likely an artefact of the use of potassium permanganate (greensand) filtration to oxidize iron and manganese out of the treated potable water.

Table 6. Pond sediment metal concentration analysis, initially measured as mg/kg and presented as percent average of two post-brine samples from each pond (P1, P2, P3, P4, P5) and total average.

	Percent Average (Post-Brine)					Total Average
	P1	P2	P3	P4	P5	
Aluminum (Al)	54.43%	13.68%	28.22%	30.07%	14.03%	28.09%
Calcium (Ca)	14.36%	53.80%	38.75%	32.11%	53.65%	38.53%
Iron (Fe)	15.37%	10.24%	11.00%	13.50%	11.41%	12.30%
Magnesium (Mg)	1.71%	4.85%	8.20%	2.07%	4.70%	4.31%
Manganese (Mn)	5.05%	6.54%	6.16%	8.77%	4.21%	6.15%
Phosphorus (P)	2.90%	1.35%	2.04%	3.41%	1.29%	2.20%
Sodium (Na)	0.99%	1.30%	0.82%	1.12%	0.88%	1.02%
Strontium (Sr)	0.69%	0.35%	0.46%	0.46%	0.33%	0.46%
Sulfur (S)	3.92%	7.45%	3.74%	8.05%	8.87%	6.40%
Total	99.41%	99.56%	99.41%	99.57%	99.37%	99.46%

The presence of strontium in small concentrations of only 0.5% is most likely due to strontium having been adsorbed to the sediments or co-precipitated with calcium. The conditions in the WTP wastewater are not such that they propagate precipitation of Sr^{2+} through strontianite or celestite (Table 4). Statistical correlation analysis was performed on the data presented in Table 6 demonstrating strong positive correlations between aluminum, iron, and strontium and strong negative correlations between calcium and aluminum, calcium and iron, and calcium and strontium in the sediments. The strong positive correlation suggests that the elements come from the same wastewater discharge source from the WTP and are not necessarily found in those quantities in natural soils.

Using PHREEQC analysis, a diffuse double-layer surface-complexation model was used to equilibrate the WTP wastewater from the pond inlet (pre-brine) with sediments/colloids in the ponds. The results suggest that calcium sorption dominates the strong sorption sites on the oxide surface, while the weak site sorption is dominated by carbonate (Table 7).

Table 7. Diffuse double-layer surface complexation model of the WTP wastewater pond inlet prior to daily brine discharge and raw water control sample from laboratory experiments.

Species	Mole Fraction	
	Pond Inlet	Raw Water (Lab Experiment)
Hfo_sOHCa ⁺²	0.622	0.590
Hfo_sOHSr ⁺²	0.003	0.002
Hfo_wCO ₃ ⁻	0.723	0.651
Hfo_wOHSO ₄ ⁻²	0.185	0.139
Hfo_wOMg ⁺	0.017	0.065

The presence of calcium in the sediments is not limited to the wastewater discharge and is also attributable to vegetation growing in the holding ponds. Vegetation decay contributes to the calcium accumulation in the sediments. The negative correlation between calcium and iron is due to the changing redox potential of the water on the bottom of the ponds as driven by microbiological action and reduced levels of oxygen. For example, decaying plants will promote biological activity at the bottom of the ponds, thereby consuming oxygen and initiating changes in redox reactions and subsequently affecting the stability of iron in the sediments resulting in redissolution into the water phase (Table 3). As the number of basic ions increases in the soils, the quantity of acidic ions decreases and vice versa. The negative correlation between calcium and aluminum occurs under the increased SAR ratio (Table 5) since aluminum cations are acidic whereas calcium ions are basic. Thus, it follows that the negative correlation between calcium and strontium is connected to the negative correlation between calcium and aluminum. Additionally, there is a moderate negative correlation between aluminum and magnesium and strontium and magnesium. The reduction of the aluminum in sediments affects the desorption of strontium by the dissolution of the calcium carbonate and/or dolomite precipitates.

Analyses of WTP holding pond wastewater and sediments show that trace minerals in any continuously discharging wastewater accumulate in the sediments and that the sediments increasingly become a source of contamination. The buildup is enhanced by particles/sediments/colloids movement in the water since they provide a bonding surface for mineral adsorption or precipitation even though there is no supersaturation of species in the water. The analyses imply that calcium-based carbonate species drive the minerals' adsorption in the presence of metal oxide particles. In that process, other minerals, such as strontium, are also removed from the water phase.

3.2. Laboratory Experiments

The results of water quality analyses for WTP wastewater experiments are presented according to the treatment of the pyrolusite media over time (Table 8). Results for both 0.5 and 6 h samples are shared alongside the control sample to which no pyrolusite media was added. The water in all experiments containing pyrolusite experienced a loss of Ca, Mg, K, Na, and Sr within the first 0.5 h (Table 8). Additional reductions were experienced by the 6 h mark for CA, Na, and Sr.

Table 8. Average water quality collection from time-series WTP wastewater experiments with pyrolusite media. Duplicate samples were collected from beakers containing untreated pyrolusite, as well as HA- and FA-pretreated pyrolusite media. Water quality results for the control sample (containing no pyrolusite) are also provided. All water quality analyses were performed by a certified analytical laboratory.

Parameters (mg/L)	Untreated 0.5 h	Untreated 6 h	HA 0.5 h	HA 6 h	FA 0.5 h	FA 6 h	Control
Conductivity ($\mu\text{S}/\text{cm}$)		4005		4.00×10^3		4.01×10^3	4.05×10^3
Bicarbonate (HCO_3)		994.5		9.86×10^2		9.82×10^2	1.06×10^3
Sulfate (SO_4)		1.65×10^3		1.63×10^3		1.65×10^3	1.65×10^3
Calcium (Ca)	3.33×10^2	3.35×10^2	3.43×10^2	3.34×10^2	3.42×10^2	3.36×10^2	3.92×10^2
Magnesium (Mg)	1.79×10^2	1.81×10^2	1.82×10^2	1.84×10^2	1.82×10^2	1.81×10^2	2.14×10^2
Potassium (K)	1.68×10^1	1.70×10^1	1.74×10^1	1.76×10^1	1.74×10^1	1.71×10^1	2.18×10^1
Sodium (Na)	4.15×10^2	4.20×10^2	4.19×10^2	4.32×10^2	4.28×10^2	4.21×10^2	5.17×10^2
Strontium (Sr)	2.67×10^0	2.63×10^0	2.72×10^0	2.64×10^0	2.74×10^0	2.63×10^0	2.91×10^0
pH		8.15×10^0		8.14×10^0		8.16×10^0	8.16×10^0
Hardness (as CaCO_3)		1.58×10^3		1.59×10^3		1.58×10^3	1.86×10^3

A reduction in alkalinity and conductivity was noted in 6 h water samples compared to the initial water quality, whereas the reduction in the sulfate concentration was small and observed in only one sample. While initial water hardness due to Ca^{2+} and Mg^{2+} was observed, the precipitation of these ions along with the carbonates resulted in lower water hardness within 0.5 h of exposure to pyrolusite. It is assumed that additional mineral loss between 0.5 and 6 h was primarily due to adsorption to those rapidly precipitated minerals in the first 0.5 h of the experiment.

As with the field samples, PHREEQC analysis was used to determine saturation indices (SI) of species in the raw water sample and 6 h untreated pyrolusite water sample (Table 4), as well as for surface adsorption (Table 7). The SI results show that calcium carbonate species and dolomite will precipitate, while that of strontianite suggests that precipitation is less likely. The rationale is that CaCO_3 will precipitate first, resulting in a loss of carbonate and consequent hindrance of strontianite precipitation. Surface adsorption results indicate that calcium dominated the adsorption to the strong site while the weak site is dominated by carbonate adsorption. Although the SI data indicate that the water is saturated with calcium carbonate species along with dolomite and will precipitate, the surface complexation model suggests that magnesium adsorption will be small compared to calcium adsorption. Dolomite ($\text{CaMg}(\text{CO}_3)_2$) formation requires equal parts of calcium and magnesium and two parts of alkalinity where calcium carbonate species form. Table 9 provides data that highlight sodium, alkalinity, calcium, and magnesium as the major elements that experienced reduced concentrations from the initial raw water quality and after contact with pyrolusite, whether treated with HA or FA or not.

Table 9. Change in concentration of water quality parameters (relative to initial raw water quality) from laboratory experiment versus control water sample (i.e., no pyrolusite media). R-untreated is the difference in concentration between raw water and average of all water samples with non-pretreated media; R-HA and R-FA are the same with media pretreated with HA or FA, respectively.

Water Quality Parameters (mg/L)	R-Untreated	R-HA	R-FA
Alkalinity, Total (as CaCO ₃)	5.35×10^1	6.10×10^1	6.40×10^1
Bicarbonate (HCO ₃)	6.55×10^1	7.45×10^1	7.80×10^1
Chloride (Cl)	5.00×10^{-1}	2.00×10^0	5.00×10^{-1}
Hardness (as CaCO ₃)	2.80×10^2	2.70×10^2	2.80×10^2
Calcium (Ca)	5.70×10^1	5.80×10^1	5.60×10^1
Magnesium (Mg)	3.35×10^1	3.05×10^1	3.35×10^1
Potassium (K)	4.85×10^0	4.20×10^0	4.75×10^0
Silicon (Si)-Dissolved	7.00×10^{-1}	5.50×10^{-1}	7.50×10^{-1}
Sodium (Na)	9.75×10^1	8.55×10^1	9.60×10^1
Strontium (Sr)-Dissolved	2.85×10^{-1}	2.75×10^{-1}	2.85×10^{-1}
Sulfate (SO ₄)-Dissolved	-5.00×10^0	1.00×10^1	-5.00×10^0

The laboratory experiment results are very similar to the results of the analysis performed on the WTP holding pond water. These results are as expected because the water source is the same. Chemical analysis of water at 3 d showed a loss of calcium, magnesium, alkalinity, sodium, and strontium across all media preparations. An ANOVA was run to determine if a significant difference exists between the precipitation of minerals relative to the adsorption on treated and untreated pyrolusite media. The ANOVA test confirms that there is no significant difference ($p > 0.05$ for Ca, Mg, Sr) across the three media treatments. Additionally, the two-sample hypothesis t-test for Ca and Sr shows that the largest precipitation of both occurs at the initial contact of water and sediments.

The precipitation of CaCO₃ was confirmed through the experiments along with confirmation that the majority of the removal of calcium, magnesium, sodium, and strontium from the aqueous phase occurred within the first 0.5 h of contact with media. While those concentrations experienced further reduction at the 6 h point, statistical analysis of the precipitates confirms that the largest reduction from the water occurred during the initial 0.5 h contact with media. This agrees with the work reported by Carteret et al. [30] where lab-induced precipitation of aragonite and vaterite was characterized by a drop in the calcium concentration. In that experiment, it was reported that precipitation occurred within 2 min with the continued transformation taking place over several days as unstable polymorphs aragonite and vaterite were transformed into more stable calcite. Littlewood et al. [31] report that at higher Sr²⁺ concentrations, Sr²⁺ was incorporated into calcite in the presence of Mg²⁺ where smaller Mg²⁺ ions compensate for the addition of the larger Sr²⁺ ions in the calcite lattice.

In addition to the analysis of water quality in response to the exposure to pyrolusite media over time, XPS analyses of six pyrolusite media samples collected at 3 h and 3 d were completed. The results point to the predominance of carbon and oxygen on the media surface, with traces of Ca, Si, Fe, Al, Mg, and S detected. XPS did not detect any Sr²⁺ on the surface of any media samples. Results from XPS analysis showed that coating the filtering media with humic (HA) or fulvic (FA) acids did not enhance the precipitation or the adsorption of Ca²⁺ or Sr²⁺ compared to the untreated media.

Both chromatographs and photoluminescence precipitate images of pyrolusite media at 0.5 h and 3 d exposure were produced using Raman Spectroscopy (Figures 4 and 5). For instance, Figure 4a illustrates the presence of sorbed precipitate on the media surface as

well as the pronounced Raman spectra peaks at 1016 cm^{-1} , then 674 cm^{-1} and 498 cm^{-1} , which identify those precipitates as calcium sulfate [32,33].

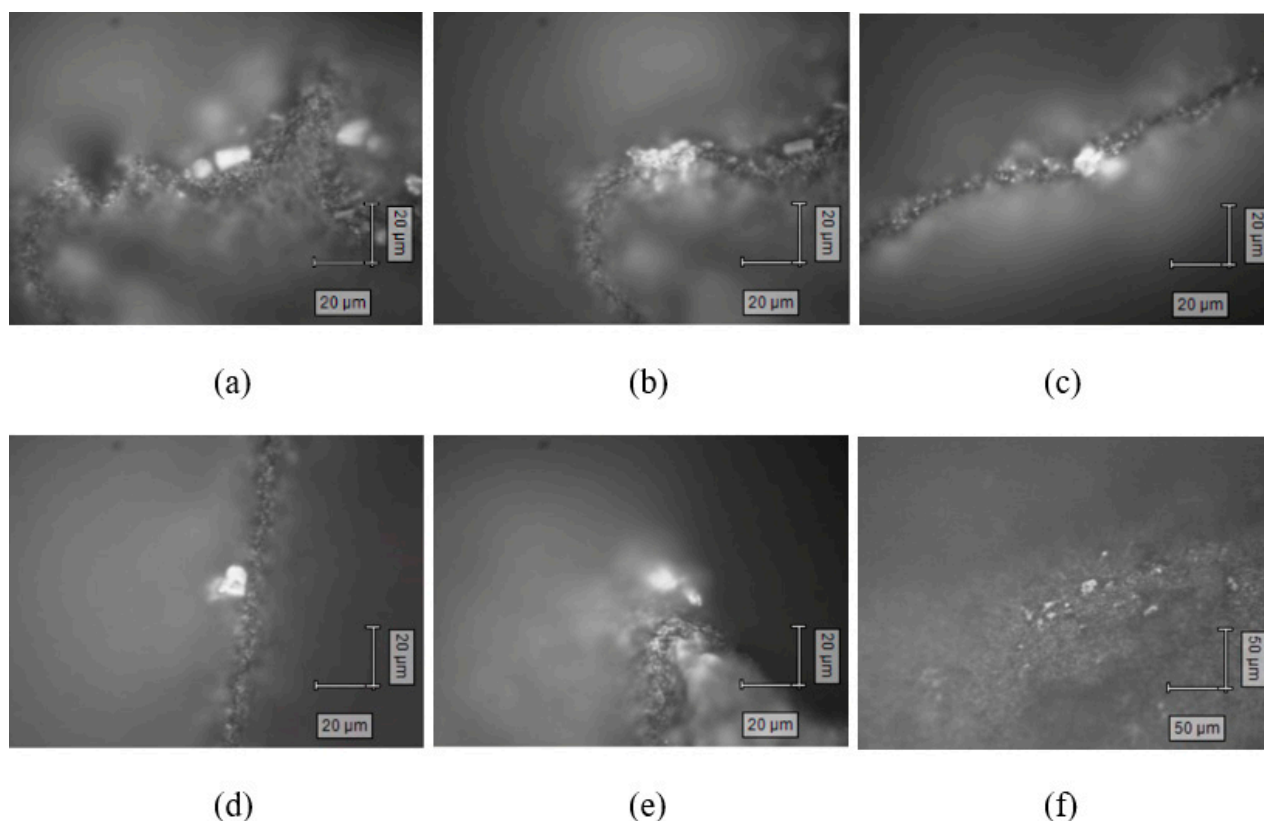


Figure 4. Crystals/precipitates showing on the surface of the media in water for 30 min and 3 days at $6\text{ }^{\circ}\text{C}$: (a) 30 min raw MnOx—CaSO₄ precipitates; (b) 30 min raw MnOx-sample 785 with CaCO₃; (c) FA 30 min; (d,e) 3-day raw MnOx—CaCO₃; (f) HA day 3.

All remaining identifiable precipitates were determined to be CaCO₃, although Figure 4c was deemed nonidentifiable due to photoluminescence interference with Raman spectral imaging. The luminescence is reflected as large bands overlaid on the Raman spectrum. The Raman spectra (Figure 5) were compared to the RRUFF database, identified by X-ray diffraction and chemical analyses. Calcite crystal R050128 was identified as a pseudomorph of aragonite while the others did not indicate the presence of aragonite. Further Raman spectra data regarding the lattice and internal vibration mode of precipitates are provided for further detail regarding precipitate chemistry (Table S1). Additional comparison spectra against the RRUFF database were also completed (Figures S1 and S2) indicating that sample R150020 was a calcite with traces of strontium (Ca_{0.993}CO₃; trace amount of strontium) as identified by X-ray diffraction and chemical analysis [29].

Comparison of the experimental results with the Raman spectra analysis from existing data from samples of aragonite, calcite, and calcite with Sr²⁺ impurities shows that graphed results from the experiment best fit the graph of calcite sample with traces of strontium captured in the lattice. The presence of strontium impurities provides one explanation for the lattice results producing a better fit with an aragonite structure than calcite as compared to the literature [30,34].

Overlaying the experimental data over the mineralogical samples data available from the RRUFF database showed that experimental data have the best fit over the RRUFF calcite sample containing strontium impurities in the lattice. Additionally, a lattice vibration showed that there were some impurities captured inside the calcite precipitate. That is, lattice vibrations suggest that calcite is not in a pure form. The wide range of absorption spectra in the lattice vibration could be due to the crystal orientation, as well as the

incorporation of ions larger than Ca into a calcite structure [35]. The pure calcite lattice vibration measures 281 cm^{-1} , while the lattice vibration of the experimental precipitates measured anywhere from 268 to 277 cm^{-1} . The shift downward suggests that molecules captured within are of a larger radius than calcium. Strontium has a larger radius than calcium. In the experiment, strontium is the only element with a radius larger than calcium that was reduced from the water. Work by Shibano et al. [27] showed that the lattice vibration of calcite with strontium as impurities measured anywhere from 281 to 273 cm^{-1} with the Sr/Ca mol ration ranging from 0 to 13.2. The higher concentration of strontium in the precipitates produced a lower wavelength due to the larger interionic distance and smaller force constants [34]. Using the wavelengths obtained by Shibano et al. [27], it was estimated that the ratio of Sr/Ca (mol) in the precipitates in this experiment was 8 to 11. As such, there is significant evidence based on this experiment accompanied by previous work of others to confirm that the strontium was captured in the precipitate, as the wavelength of the lattice vibration suggests. In the precipitates from this experiment, it is possible that the Sr^{2+} was most likely positioned in the center of the precipitate and less likely toward the edge and that is why XPS did not detect any strontium on the surface of the precipitate.

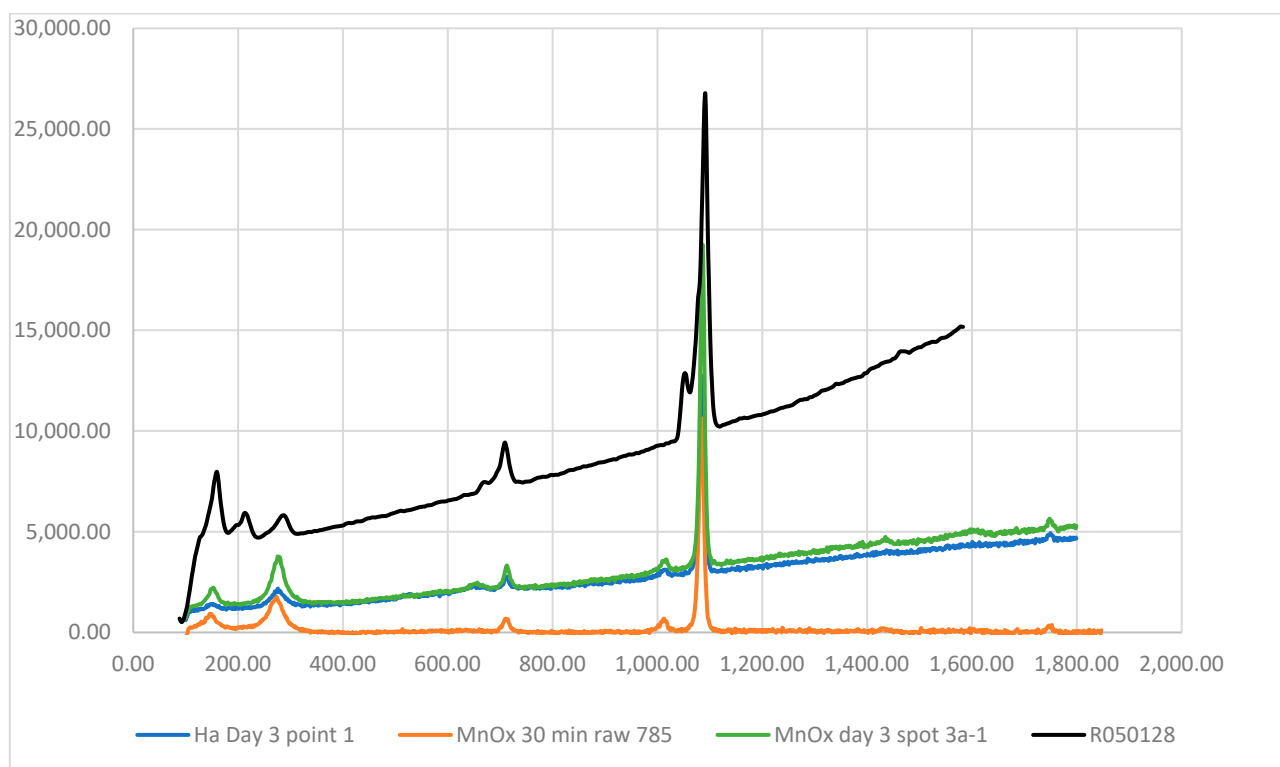


Figure 5. Sample R050128 (RRUFF, 2015) is a calcite, not a single crystal, with aragonite traces still present (black); HA Day 3 point 1 sample (blue) is a precipitate on the media pretreated with haloacetic acid where media is submerged in water for 3 days; MnOx 30 min raw 785 (orange) where media was not pretreated and was submerged for 30 min; sample MnOx 3 day spot 3a-1 media was not pretreated with anything and was submerged for 3 days (green).

4. Conclusions

The experimental observations of strontium co-precipitation from WTP wastewater show that, once discharged to an aquatic receiving environment, a loss of dissolved strontium from water is expected and can be quantified. Quantification of the radionuclide precipitation is particularly important for safety assessment studies over a wide range of conditions. Assessment of the impact of the discharge should start by assessing the dispersion and accumulation of radionuclides in environmental materials as a function of time and distance from the source. Experiments performed in this study showed that Sr^{2+}

precipitation occurred along with calcite, a CaCO_3 polymorph, at 6 °C. The water quality data analysis shows that the declining concentration of Sr^{2+} , Ca^{2+} , and bicarbonate in the aqueous phase occurred quickly and in agreement with previously published literature. Precipitates were observed to form and sorb in response to exposure to pyrolusite media in WTP wastewater. It was also observed that larger precipitate crystals may form due to prolonged contact between the water and pyrolusite. Therefore, it was concluded that waters with scaling capacity will precipitate CaCO_3 and other impurities, such as Sr^{2+} . Strontium sorption onto the sediments associated with those waters will continue to occur predominantly with calcite co-precipitation. As the water interacts with media particles/sediments that provide a surface for the precipitate to attach itself, precipitation will continue until the water quality achieves equilibrium. Understanding the mechanism of strontium loss from natural waters can assist in establishing a robust monitoring approach of ^{90}Sr deposition in the event of an unplanned release from the eventual operation of nuclear-fueled power plants in the region.

Supplementary Materials: The following supporting information can be downloaded at: <https://www.mdpi.com/article/10.3390/environments9060072/s1>, Table S1: Raman spectroscopy of reference samples and samples collected in this work; Figure S1: Sample R050127 is a pure calcite (light red), HA Day 3 point 1 sample (blue) is a precipitate on the media pretreated with haloacetic acid where media was submerged in water for 3 days, MnOx 30 min raw 785 (orange) where media was not pretreated and was submerged for 30 min, sample MnOx 3 day spot 3a-1 media was not pretreated with anything and was submerged for 3 days (green); Figure S2: Sample R050020 is a calcite with 99.3% of calcium and trace amounts of strontium (dark red), HA Day 3 point 1 sample (blue) is a precipitate on the media pretreated with haloacetic acid where media was submerged in water for 3 days, MnOx 30 min raw 785 (orange) where media was not pretreated and was submerged for 30 min, sample MnOx 3 day spot 3a-1 media was not pretreated with anything and was submerged for 3 days (green).

Author Contributions: The research concept was co-conceived by the authors, and experimental and empirical model development and validation were completed by E.Z. The authors contributed equally to the preparation of this manuscript. All authors have read and agreed to the published version of the manuscript.

Funding: This research was funded by the Sylvia Fedoruk Canadian Centre for Nuclear Innovation and the Natural Sciences and Engineering Research Council of Canada (NSERC) (DWM 2020-04014).

Institutional Review Board Statement: Not applicable.

Informed Consent Statement: Not applicable.

Data Availability Statement: Not applicable.

Conflicts of Interest: The authors declare no conflict of interest.

References

1. Salbu, B.; Skipperud, L. *Nuclear Risk in Central Asia*; Salbu, B., Skipperud, L., Eds.; NATO Science for Peace and Security Series; Springer: Dordrecht, The Netherlands, 2008; ISBN 978-1-4020-9317-4.
2. Sunderman, D.N.; Townley, C.W. *The Radiochemistry of Barium, Calcium, and Strontium*; Report NAS-NS 3010; National Academy of Sciences: Washington, DC, USA; National Research Council: Washington, DC, USA, 1960. Available online: <https://www.osti.gov/servlets/purl/4140481> (accessed on 15 October 2021).
3. Tu, Y.-J.; You, C.-F.; Zhang, Z.; Duan, Y.; Fu, J.; Xu, D. Strontium Removal in Seawater by Means of Composite Magnetic Nanoparticles Derived from Industrial Sludge. *Water* **2016**, *8*, 357. [[CrossRef](#)]
4. Carroll, S.A.; Roberts, S.K.; Criscenti, L.J. Surface complexation model for strontium sorption to amorphous silica and goethite. *Geochem. Transp.* **2008**, *9*, 2. [[CrossRef](#)] [[PubMed](#)]
5. Salbu, B.; Lind, O.C. Analytical techniques for characterizing radioactive particles deposited in the environment. *J. Environ. Radioact.* **2019**, *211*, 106078. [[CrossRef](#)]
6. Salbu, B.; Skipperud, L. Speciation of radionuclides in the environment. *J. Environ. Radioact.* **2009**, *100*, 281. [[CrossRef](#)]
7. Bush, E.; Lemmen, D.S. *Canada's Changing Climate Report*; Government of Canada: Ottawa, ON, Canada, 2019; ISBN 978-0-660-30222-5.

8. Loeppky, A.; Anderson, W. Environmental influences on uptake kinetics and partitioning of strontium in age-0 lake sturgeon (*Acipenser fulvescens*): Effects of temperature and ambient calcium activities. *Can. J. Fish. Aquat. Sci.* **2021**, *78*, 612. [CrossRef]
9. Mirzoeva, N.; Shadrin, N.; Arkhipova, S.; Miroshnichenko, O.; Kravchenko, N.; Anufrieva, E. Does Salinity Affect the Distribution of the Artificial Radionuclides ^{90}Sr and ^{137}Cs in Water of the Saline Lakes? A Case of the Crimean Peninsula. *Water* **2019**, *12*, 349. [CrossRef]
10. Jabbar, T.; Wallner, G. Biotransformation of Radionuclides: Trends and Challenges. In *Radionuclides in the Environment*; Walther, C., Gupta, D., Eds.; Springer: Cham, Switzerland, 2015. [CrossRef]
11. Salbu, B.; Kashparov, V.; Lind, O.C.; Garcia-Tenorio, R.; Johansen, M.P.; Schild, D.P.; Roos, P.; Sancho, C. Challenges associated with the behavior of radioactive particles in the environment. *J. Environ. Radioact.* **2017**, *186*, 101. [CrossRef] [PubMed]
12. Marques, J.M.; Carreira, P.M. The use of environmental isotopes in groundwater studies with hydrogeothics: Essential or dispensable? *Sustain. Water Resour. Manag.* **2022**, *8*, 74. [CrossRef]
13. Barbieri, M. Isotopes in Hydrology and Hydrogeology. *Water* **2019**, *11*, 291. [CrossRef]
14. Zheleznyak, M.; Donchytz, G.; Hygynyak, V.; Marinets, A.; Lyashenko, G.; Tklich, P. RIVOTOX-one dimensional model for the simulation of the transport of radionuclides in a network of river channels. In *RODOS Report Decision Support for Nuclear Emergencies*; RODOS-WG4-TN(97)05; Forschungszentrum Karlsruhe: Karlsruhe, Germany, 2003.
15. International Atomic Energy Agency (IAEA). *Quantification of Radionuclide Transfer in Terrestrial and Freshwater Environments for Radiological Assessments*; IAEA-TECDOC-1616; IAEA: Vienna, Austria, 2009; Available online: https://www-pub.iaea.org/MTCD/Publications/PDF/te_1616_web.pdf (accessed on 15 October 2021).
16. Shoedarto, R.M.; Tada, Y.; Kashiwaya, K.; Koike, K.; Iskandar, I.; Malik, D.; Bratakusuma, B. Investigation of meteoric water and parent fluid mixing in a two-phase geothermal reservoir system using strontium isotope analysis: A case study from Southern Bandung, West Java, Indonesia. *Geothermics* **2021**, *94*, 102096. [CrossRef]
17. Boschetti, T.; Awaleh, M.O.; Barbieri, M. Waters from the Djiboutian Afar: A Review of Strontium Isotopic Composition and a Comparison with Ethiopian Waters and Red Sea Brines. *Water* **2018**, *10*, 1700. [CrossRef]
18. Jonker, G.S. The Removal of Radiostrontium by Precipitation. Ph.D. Thesis, Delft University of Technology, Delft, The Netherlands, 1976. Available online: https://inis.iaea.org/collection/NCLCollectionStore/_Public/07/263/7263684.pdf (accessed on 15 October 2021).
19. McCauley, R.F.; Eliassen, R. Radioactive-Strontium Removal by Lime-Soda Softening. *J. Am. Water Work. Assoc.* **1956**, *47*, 494–502. Available online: <https://www.jstor.org/stable/41254081> (accessed on 15 October 2021). [CrossRef]
20. Cooper, C.D.; Morse, J.W. Biogeochemical controls on trace metal cycling in anoxic marine sediments. *Environ. Sci. Technol.* **1998**, *32*, 327. [CrossRef]
21. Statistics Canada. Census Profile 2016: Northern [Economic Region], Saskatchewan and Saskatchewan [Province]. 2020. Available online: <https://www12.statcan.gc.ca/census-recensement/index-eng.cfm> (accessed on 15 October 2021).
22. Health Canada. Strontium in Drinking Water—Guideline Technical Document for Public Consultation. 2018. Available online: <https://www.canada.ca/en/health-canada/programs/consultation-strontium-drinking-water/document.html> (accessed on 15 October 2021).
23. Environment and Climate Change Canada (ECCC). Federal Environmental Quality Guidelines—Strontium. 2020. Available online: <https://www.canada.ca/en/environment-climate-change/services/evaluating-existing-substances/federal-environmental-quality-guidelines-strontium.html> (accessed on 15 October 2021).
24. Water Security Agency of Saskatchewan (WSASK). Surface Water Quality Data. 2013. Available online: <https://www.saskatchewan.ca/residents/environment-public-health-and-safety/environmental-health/water-and-wastewater-management/water-quality-information> (accessed on 15 October 2021).
25. Dzombak, D.A.; Morel, F.M.M. *Surface Complexation Modeling: Hydrous Ferric Oxide*; Wiley: Hoboken, NJ, USA, 1991; ISBN 978-0-471-63731-8.
26. Dandeu, A.; Humbert, B.; Carteret, C.; Muhr, H.; Plasarim, E.; Bossoutrot, J.M. Raman Spectroscopy—A Powerful Tool for the Quantitative Determination of the Composition of Polymorph Mixtures: Application to CaCO_3 Polymorph Mixtures. *Chem. Eng. Technol.* **2006**, *29*, 221. [CrossRef]
27. Shibano, Y.; Takahata, K.; Kawano, J.; Watanabe, T.; Enomoto, D.; Kagi, H.; Kamiya, N.; Yamamoto, J. Raman spectroscopic determination of Sr/Ca ratios of calcite samples. *J. Raman Spectrosc.* **2017**, *48*, 1755. [CrossRef]
28. Kaabar, W.; Bott, S.; Devonshire, R. Raman spectroscopic study of mixed carbonate materials. *Spectrochim. Acta* **2011**, *A78*, 136. [CrossRef] [PubMed]
29. RRUFF. The RRUFF™ Project. 2015. Available online: <https://rruff.info/> (accessed on 15 October 2021).
30. Carteret, C.; Dandeu, A.; Moussaoui, S.; Humbert, B.; Plasari, E. Polymorphism studied by lattice phonon Raman Spectroscopy and Statistical Mixture Analysis Method. Application to Calcium Carbonate polymorphs during batch crystallization. *Cryst. Growth Des.* **2008**, *9*, 807. [CrossRef]
31. Littlewood, J.L.; Shaw, S.; Peacock, C.L.; Bots, P.; Trivedi, D.; Burke, I.T. Mechanism of Enhanced Strontium Uptake in Calcite via an Amorphous Calcium Carbonate Crystallization Pathway. *Cryst. Growth Des.* **2017**, *17*, 1214. [CrossRef]
32. Buzgar, N.; Buzatu, A.; Sanislav, I.V. The Raman Study on Certain Sulfates. *Analele Științifice Ale Universității “AL. I. CUZA” IAȘI*. Corpus ID: 67770763. 2009, Volume 55. Available online: http://geology.uaic.ro/aug/articole/2009%20no1/1_L01-Buzgar%20-%20pag%205-23.pdf (accessed on 15 October 2021).

33. Liu, Y.; Wang, A.; Freeman, J.J. Raman, MIR, and NIR spectroscopic study of calcium sulfates: Gypsum, bassanite, and anhydrite. In Proceedings of the 40th Lunar and Planetary Science Conference, The Woodlands, TX, USA, 23 March 2009; Available online: <https://www.lpi.usra.edu/meetings/lpsc2009/pdf/2128.pdf> (accessed on 15 October 2021).
34. Krishnamurti, D. The Raman Spectra of Aragonite, Strontianite and Witherite. *Proc. Indian Acad. Sci.* **1960**, *51*, 285. [[CrossRef](#)]
35. Alía, J.M.; de Mera, Y.D.; Edwards, H.G.M.; Martín, P.G.; Andrés, S.L. FT-Raman and infrared spectroscopic study of aragonite-strontianite (Ca_xSr_{1-x}CO₃) solid solution. *Spectrochim. Acta Part A Mol. Biomol. Spectrosc.* **1997**, *53*, 2347. [[CrossRef](#)]